Effect of cation sizes on tunnelling states, relaxations and anharmonicity of alkali borate glasses

2006 J. Phys.: Condens. Matter 18 3251

(http://iopscience.iop.org/0953-8984/18/12/007)

INSTITUTE OF PHYSICS PUBLISHING JOURNAL OF PHYSICS: CONDENSED MATTER

J. Phys.: Condens. Matter **18** (2006) 3251–3262 doi:10.1088/0953-8984/18/12/007

Effect of cation sizes on tunnelling states, relaxations and anharmonicity of alkali borate glasses

Giovanni Carini[1], Giuseppe Carini[1], Gaspare Tripodo[1], Antonio Bartolotta[2] and Gaetano Di Marco[2]

[1] Dipartimento di Fisica, Università di Messina, Salita Sperone 31, I-98166 S Agata, Messina, Italy
[2] Istituto per i Processi Chimico-Fisici del CNR, Sezione di Messina, Via La Farina 237, I-98123 Messina, Italy

Received 20 January 2006
Published 7 March 2006
Online at stacks.iop.org/JPhysCM/18/3251

Abstract

The relaxation losses and the corresponding velocity variations, observed at ultrasonic frequencies in $(M_2O)_{0.14}(B_2O_3)_{0.86}$ alkali borate glasses (M = Li, K, Cs) between 1.5 and 300 K, have been modelled by an asymmetric double-well potential model having a distribution of both the barrier potential and the asymmetry. It is shown that the relaxation strength C^* and the spectral density of asymmetries f_0 decreases markedly with decreasing cation size. Below 10 K the sound attenuation is regulated by the phonon-assisted relaxation of tunnelling systems and exhibits a tunnelling strength C, ranging between 10^{-4} and 10^{-3}. At variance with the behaviour observed for C^*, C slightly increases with decreasing cation size and is more than one order of magnitude smaller than C^*. It is concluded that, differently from classical relaxing states, tunnelling systems are independent of bond strengths and of structural changes characterizing a glassy network, confirming their inherent universality. Above about 120 K the ultrasonic velocity is mainly regulated by vibrational anharmonicity and shows a nearly linear decrease as the temperature is increased, the slope scaling with the cation size. Taken together, the observations point to the existence of a distinct correlation between anharmonicity and local mobility in the glassy network.

1. Introduction

The origin and the nature of low energy excitations is a central question in the physics of disordered solids. They are responsible for anomalies in the thermal [1, 2] and acoustic [3, 4] properties of glasses in the low temperature regions both below and above 1 K and are usually accounted for by local motions of localized structural defects. The tunnelling model [5, 6] associates these defect modes with single atoms or groups of atoms subjected to quantum-mechanical tunnelling between two different stable positions available in the glassy network, and schematizes the locally mobile 'particles' by asymmetric double-well potentials. A more recent extension of the tunnelling model [7, 8] includes the case of a strong coupling between

tunnelling two-level systems (TLS) and phonons and individuates three temperature regions where different mechanisms are regulating the motion within the two wells and the related acoustic properties: coherent tunnelling at low temperatures ($T < 5$ K), incoherent tunnelling at intermediate temperatures (5 K $< T <$ 20 K) and thermally activated jumps over the potential barrier at higher temperatures ($T > 20$ K). This theoretical approach covers both tunnelling and classical activation, leading to a coherent description of the acoustic behaviours of glasses over the wide range from very low temperatures to room temperature. It has been proved, in fact, that theoretical evaluation of the acoustic attenuation in the kHz range permits the reproduction, with good or acceptable agreement, of the behaviours observed in glassy GeO_2 and B_2O_3 [8].

A very recent study of the acoustic attenuation over the MHz range in Li_2O–B_2O_3 borate glasses [9] gave strong indications that only a small fraction of the thermally activated relaxing particles are involved in tunnelling local motions below 10 K. Moreover, at variance with the trend following from the concentration of relaxing defects, the TLS spectral density turns out to be independent of the structural changes due to variations in the Li_2O concentration. In that case a symmetric double-well potential model with a broad Gaussian distribution of barrier heights was used to account for the relaxation losses, so that only a rough comparison between the numerical densities of both the tunnelling and the relaxing centres was possible. It is the purpose of the present paper to improve the previous analysis by applying the asymmetric double-well potential (ADWP) model [10, 11] to explain the low temperature secondary loss peaks and the corresponding velocity variations observed in glasses. In the ADWP model the underlying relaxation processes are interpreted by assuming the existence of intrinsic defects subjected to thermally activated local motions within asymmetric double-well potentials. The double-well potentials have broad distributions of both barrier height V and asymmetry Δ, which are considered as independent variables. As in the tunnelling model, the ultrasonic strain interacts with the relaxing defects by modulation of the asymmetry Δ, so that application of this model permits us to obtain a direct link between the microscopic mechanisms, low temperature tunnelling and high temperature classical activation regulating the acoustic behaviours in a glass. In addition to this the relation between TLS, the structural defects and the nature of the bonding in the glassy network has been explored by analysing the acoustic properties of $(M_2O)_{0.14}(B_2O_3)_{0.86}$ borate glasses, where M corresponds to Li, K and Cs, i.e. alkaline cations having increasing sizes. Since the borate host matrix preserves the main features of the local structure at a fixed concentration of monovalent network modifier ions (NMI) in the range of molar fractions $X \leqslant 0.20$ [12–16], changes in the number or in the local mobility of the structural defects should be ascribed to differences in the bond strength of NMI. This specific composition was selected in order to avoid the formation of non-bridging oxygens which could give rise to undesired contributions to the acoustic behaviours and also to ensure a sufficient number of NMI in the glassy network to observe significant changes in the local mobility.

The results suggest that the polarizing power of the ion modifying the host structure markedly affects the population of classical relaxing defects and the anharmonicity of these borate glasses, but leaves unaltered some typical features of TLSs as a further indication of their inherent universality. Furthermore it has been revealed that the low temperature tunnelling strength C is more than one order of magnitude lower than the high temperature relaxation strength C^*.

2. Experimental details

$(M_2O)_{0.14}(B_2O_3)_{0.86}$ glasses, where M corresponds to Li, K or Cs, were prepared and characterized (room temperature densities and linear thermal expansion coefficients between 100 and 300 K) following the same specific procedures already described [9].

The specific heat capacity and the glass transition temperatures T_g of the samples were determined by the thermograms measured by a Perkin Elmer differential scanning calorimeter (DSC-Pyris). Discs of each glass of mass approximately 15 mg were encapsulated in aluminium pans and subjected to the same thermal cycles from 300 K to about 700–800 K (depending on their T_g) with a heating rate of 20 K min^{-1}. Calibration of the DSC output was performed using a standard sapphire sample.

The attenuation and velocity of longitudinal and shear ultrasonic waves were measured between 1.5 and 300 K using a conventional pulse-echo ultrasonic technique in the 10–70 MHz frequency range [9].

3. Experimental results

To illustrate the effects of changing the NMI, the experimental results for the temperature dependence of the attenuation of 50 MHz ultrasonic waves for $(M_2O)_{0.14}(B_2O_3)_{0.86}$ glasses were transformed into the internal friction Q^{-1} ($=0.23\alpha_{db}v/\omega$, where α_{db} is the attenuation in db cm^{-1}, v is the sound velocity and ω the angular frequency) and are reported in figure 1(a). When the acoustic attenuation is expressed in terms of Q^{-1}, in fact, the values corresponding to the plateau, $Q^{-1}_{plateau}$, and to the maximum of the loss peak, Q^{-1}_{peak}, allow for a first rough evaluation of the tunnelling strength C (see equation (1), section 4.1) and of the relaxation strength C^* (see equation (4), section 4.1), respectively. It can be seen that, with increasing cation size from Li^+, through K^+, to Cs^+, $Q^{-1}_{plateau}$ (order of magnitude of 10^{-4}) does not show significant variations while a relevant increase occurs in Q^{-1}_{peak} (order of magnitude of 10^{-3}) as well the temperature position of the loss peak. Attenuation measurements performed for both longitudinal and shear ultrasonic waves show that, as previously observed in lithium borate glasses [9], the internal friction for both modes is about the same in the whole temperature range explored.

The Arrhenius behaviour in the plot of the frequencies versus the reciprocal temperatures of the acoustic loss maxima $(T_{peak})^{-1}$ gives the following values for the average activation energy E_{act} and the characteristic frequency τ_0^{-1} of $(M_2O)_{0.14}(B_2O_3)_{0.86}$ glasses: $E_{act}/k_B = 587$ K and $\tau_0^{-1} = 2.23 \times 10^{13}$ s^{-1} for M = Li; $E_{act}/k_B = 683$ K and $\tau_0^{-1} = 1.24 \times 10^{13}$ s^{-1} for M = K; $E_{act}/k_B = 765$ K and $\tau_0^{-1} = 2.88 \times 10^{13}$ s^{-1} for M = Cs.

The experimental data of longitudinal sound velocity at 10 MHz between 2 and 300 K, plotted as $v_l(T)/v_{l,rt}$ ($v_{l,rt}$ being the sound velocity at room temperature), are reported in figure 1(b). In all the borate glasses investigated there is a slow decrease between 2 and 7 K followed by a continuously changing slope for temperatures varying in the interval between about 10 and 120 K and a nearly linear trend for higher temperatures. Also the velocities of shear ultrasonic waves show very similar temperature behaviours. The decrease at low temperatures as the temperature is increased up to about 120 K becomes increasingly smaller on going from $(Cs_2O)_{0.14}(B_2O_3)_{0.86}$ to $(Li_2O)_{0.14}(B_2O_3)_{0.86}$ glass. The same trend is observed in the region of temperatures above 120 K, where the slope of the linear behaviour decreases markedly on going from pure B_2O_3, through $(Cs_2O)_{0.14}(B_2O_3)_{0.86}$ and $(K_2O)_{0.14}(B_2O_3)_{0.86}$, to $(Li_2O)_{0.14}(B_2O_3)_{0.86}$.

4. Discussion

4.1. Acoustic attenuation

The ultrasonic attenuation α or, equivalently, the internal friction Q^{-1} as a function of temperature for these alkali borate glasses show distinct features characteristic of many oxide glasses:

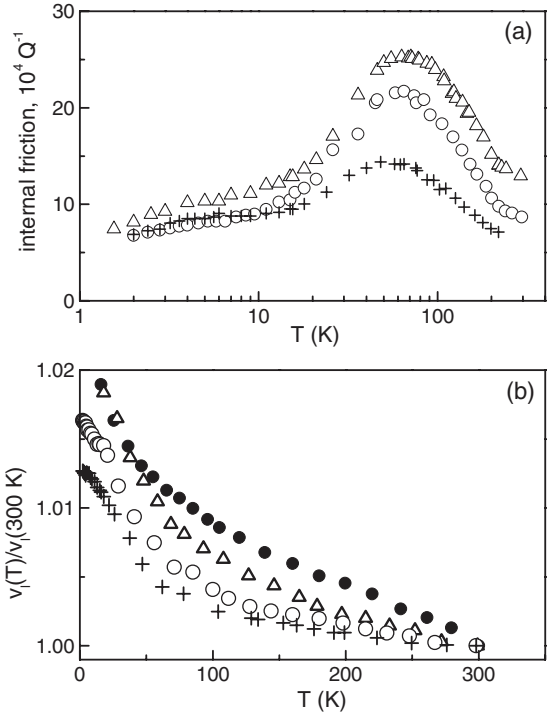

Figure 1. (a) Comparison between the internal friction Q^{-1} for longitudinal 50 MHz ultrasonic waves in $(M_2O)_{0.14}(B_2O_3)_{0.86}$ glasses: (△), M = Cs; (○), M = K; (+), M = Li. (b) Temperature dependence of the fractional sound velocity $\frac{V_l(T)}{V_{l,rt}}$ of 10 MHz longitudinal ultrasonic waves in $(M_2O)_{0.14}(B_2O_3)_{0.86}$ glasses: (●), pure B_2O_3; (△), M = Cs; (○), M = K; (+), M = Li.

(i) From 1.5 K up to about 8 K, Q^{-1} increases with increasing temperature and becomes temperature independent above 3 K at 50 MHz, the onset of the plateau shifting to higher temperatures with increasing frequency (figure 1(a)). These observations are in agreement with the predictions by Jäckle [17] from his theoretical study of the phonon-assisted tunnelling of two-level systems and subsequently also obtained within the framework of SPM [18].

(ii) In the temperature region between the plateau and the loss peak, the increase of Q^{-1} is mainly governed by a mechanism of incoherent tunnelling within the two wells because the increasing thermal motion prevents the phase coherence of the TLS tunnelling motion. It has been clearly proved [7, 8], in fact, that the predominance of this mechanism between about 5–6 and 20 K accounts for the observed increase in the attenuation in glassy SiO_2, B_2O_3 and GeO_2.

(iii) For $T > 20$ K, the thermally activated relaxations of structural defects over the potential barriers become dominant and determine the attenuation and the loss peak.

Since we are mainly concerned with the relationship between TLSs and relaxing centres, in the following we will carry out a numerical evaluation of the experimental internal friction in regions (i) and (iii), where the contribution due to incoherent tunnelling effects can be neglected.

In the plateau region the internal friction is given by [17]

$$Q_i^{-1} = \frac{\pi}{2}\left[\frac{\bar{P}\gamma_i^2}{\rho V_i^2}\right] = \frac{\pi}{2}C_i. \tag{1}$$

Here C_i is the tunnelling strength, V_i the ultrasonic wave velocity, γ_i the deformation potential that expresses the coupling between the ultrasonic stress and the system, $\bar{P}$ the TLS spectral density, ρ the sample density and the index i refers to the different polarizations (l stands for longitudinal and t for transverse). The influence of other interactions, which could lead to ultrasonic attenuation in this range of temperature, has been examined using the procedure described in detail in [19] and can be discarded. The obtained values of C_l and of the product $\bar{P}\gamma_i^2$ (reported in table 2) show a clear trend of decrease with increasing cation size. It is worth noting that the longitudinal tunnelling strengths C_l show a magnitude ranging between 10^{-3} and 10^{-4}, as universally observed in almost all the glasses [4].

In the framework of the ADWP model, the high temperature internal friction ($T > 20$ K) is given by [10, 11]:

$$Q_i^{-1} = \frac{\gamma_i^2}{\rho V_i^2 k_B T}\int\int \mathrm{d}\Delta\,\mathrm{d}V f(\Delta)g(V)\,\mathrm{sec}\,h^2\left(\frac{\Delta}{2k_B T}\right)\frac{\omega\tau}{1+\omega^2\tau^2}. \tag{2}$$

In equation (2), $f(\Delta)$ and $g(V)$ are the distributions of the asymmetries Δ and the barrier heights V and τ is the relaxation time given by

$$\tau = \tau_0 \exp\left(\frac{V}{k_B T}\right)\mathrm{sec}\,h\left(\frac{\Delta}{2k_B T}\right) \tag{3}$$

where the characteristic frequency τ_0^{-1} (related to the vibrational frequency of the particle in a single well [20]) has been assumed to be single valued.

Following Gilroy and Phillips [11], i.e. using for $g(V)$ an exponential form, $g(V) = V_0^{-1}\exp(-\frac{V}{V_0})$, and taking $f(\Delta)$ as a constant f_0, the relaxation time can be approximated by the usual Arrhenius law with V_0 as the activation energy and equation (2) can be reduced to the following analytical expression:

$$Q_i^{-1} = \pi\left(\frac{f_0\gamma^2}{\rho v^2}\right)a(\omega\tau_0)^a = \pi C^* a(\omega\tau_0)^a \tag{4}$$

where C^* is the relaxation strength and $a = \frac{k_B T}{V_0} = \frac{T}{T_0}$. Evaluation of the acoustic loss by equation (4) is given within an error of a few per cent, when $a < 0.3$ ($T < 0.3T_0$) and $\omega\tau_0 \ll 1$ (as usual in the ultrasonic range) [11].

From the data analysis the values of C^*, V_0 and τ_0^{-1} were obtained by least-squares fits of the results using a Minuit minimum search program. A typical fit of the relaxation loss is shown by a solid line in figure 2(a) and the relaxation parameters, resulting from this analysis, are given in table 2. The good fit to the shape of the experimental results and the finding that the theoretical parameters obtained from the fits to the experimental data at various frequencies are the same within a few per cent demonstrate the validity of this theoretical approach. The internal friction data have also been evaluated numerically by using equation (2) with the same constant distribution of asymmetries f_0 and a Gaussian form for $g(V)$, $g(V) = \frac{1}{\sqrt{2\pi}}V_0^{-1}\exp(-\frac{V^2}{2V_0^2})$. Using the same values of C^*, V_0 and τ_0^{-1} determined by fitting with an exponential distribution (see table 2), the curve reported as a dotted line in figure 2(a) has been obtained. It agrees with ultrasonic data in the low temperature region only, showing significant deviations from the experimental behaviour at high temperatures. This is the result of a Gaussian distribution which decreases more rapidly than the exponential one with increasing barrier height V. We want to remark, however, that the magnitude of loss

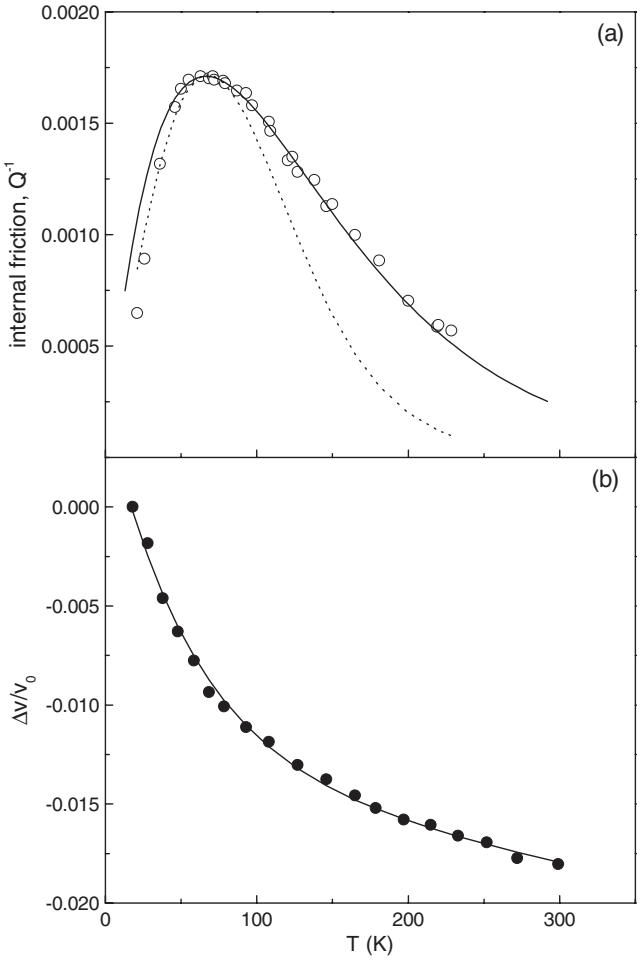

Figure 2. (a) Comparison of the experimental data for the internal friction at 50 MHz across the broad relaxation peak and the theoretical fits with the exponential (continuous line) and Gaussian (dotted line) distributions of potential barrier heights for $(Cs_2O)_{0.14}(B_2O_3)_{0.86}$. (b) Comparison of the temperature dependence of the fractional sound velocity of 10 MHz longitudinal ultrasonic waves in $(Cs_2O)_{0.14}(B_2O_3)_{0.86}$ glass and the theoretical curve (continuous line) obtained by the relaxation and anharmonic contributions evaluated using equations (7) and (8), respectively.

peak has been well reproduced by using the same value of the relaxation strength for both the distributions, a clear indication that C^* is not very sensitive to the exact form of the distribution functions. The use of less approximated expressions [21], which extend the validity of the model up to $a < 1$ (i.e. to a wide temperature range), did not produce any real improvement of the theoretical fit to the experimental data.

The activation energy V_0 does not exhibit any definite variation with increasing cation size, suggesting that the local arrangement of the relaxing particles is not greatly influenced by changing the network modifier ions. The striking feature of the results is that the relaxation strength C^*, involving the spectral density f_0 of asymmetries and the deformation potential γ_l, turns out to be more than one order of magnitude larger than the tunnelling strength C.

Using the values of C^* and those of γ_l, an order of magnitude of 10^{46} J^{-1} m^{-3} is calculated for the spectral density of asymmetries f_0, which decreases with decreasing NMI size from 15.3×10^{46} J^{-1} m^{-3} in pure B_2O_3 to 3.3×10^{46} J^{-1} m^{-3} in lithium borate glass (see table 2). The deformation potentials for $(M_2O)_{0.14}(B_2O_3)_{0.86}$ glasses were deduced by using the same procedure already described [9], i.e. linear interpolation from the plot of the values of γ_l experimentally determined in lithium borate glasses versus the corresponding glass transition temperatures T_g. Assuming that the distribution $f(\Delta)$ is equal to f_0 below V_0 and zero above, the calculated number of relaxing particles (order of magnitude of 10^{26} m^{-3}) decreases by going from pure B_2O_3 to $(M_2O)_{0.14}(B_2O_3)_{0.86}$, also exhibiting a marked decrease with decreasing cation size. Since FTIR (Fourier transform infrared) analysis of the glasses studied here revealed no sign of OH groups within experimental accuracy, it is reasonable to exclude these extrinsic defects as the origin of the observed relaxation losses [9]. Therefore the evidence above mainly supports an association between the structural relaxations and the BO_3 groups making up the skeleton of vitreous borate, because pure glassy B_2O_3 has a structure constructed from $B\text{Ø}_3$ groups (Ø=bridging oxygen atom) and the addition of alkali oxide converts these units to tetrahedral $B\text{Ø}_4^-$ groups at a rate $R = X/(1 - X)$. Moreover, the decrease of f_0 with decreasing cation size should be ascribed to variations in the polarizing power of different NMIs because, at the fixed $X = 0.14$ concentration of alkali oxide, the relative concentrations of both $B\text{Ø}_3$ and $B\text{Ø}_4$ groups are also fixed independently of the kind of NMI [12]. As shown by the plots reported in figures 3(a) and (b), the spectral density of asymmetries f_0, such as the linear expansion coefficient α_{th}, scales roughly linearly with the field strength of NMIs. The cationic field strength is given by q/r^2, q being the formal charge and r the Shannon ionic radius for typical coordinations [22]. It is believed that the Coulombic interactions between the modifying cations and the charged $B\text{Ø}_4^-$ tetrahedrons lead to a reduction in the number of internal degrees of freedom of these units, hindering their local motions between different configurations. The effect of these interactions becomes increasingly larger with growing field strength (or with decreasing cation size), enhancing the degree of hindering and causing the observed decrease in the number of relaxing units. The very close similarity between the field strength behaviours of both f_0 and α_{th} implies that the Coulombic interactions between NMIs and the charged $B\text{Ø}_4^-$ tetrahedrons impose severe restrictions on the expansion capability of the network, also preventing its local molecular mobility.

In the low temperature tunnelling region below about 8 K the effect of decreasing cation size on both $\bar{P}\gamma_l^2$ and $\bar{P}$ is to cause a slight increase in their value (table 2), in clear contrast with the decrease obtained for both $f_0\gamma_l^2$ and f_0. In addition to this, there is also a difference of more than one order of magnitude between $\bar{P}$ and f_0 which reflects the difference between quantities directly determined by experimental data: the tunnelling strength C and the relaxation strength C^*, in fact, can be derived through the values of $Q^{-1}_{plateau}$ and Q^{-1}_{rel} (see figure 1(a)) after subtraction of the low temperature background.

There were some indications [23] of a correlation existing between the tunnelling parameters Δ and $\lambda = d\sqrt{\frac{2m_0V}{\hbar^2}}$, m_0 being the effective mass of the tunnelling particle and d the distance between the two wells, which should lead to a relation between Δ and V, the parameters of the ADWP. The present results do not give the opportunity of testing the result of that theoretical analysis because more accurate information about the microscopic nature and the kind of local motion of the defects is at present lacking. More experiments on glasses are necessary to prove the existence of the proposed correlation. As an example, application of increasing pressure to a glass is expected to cause changes in both the asymmetry and the barrier height of the ADWP and, consequently, acoustic experiments as a function of temperature and pressure could help to obtain an insight into the above question.

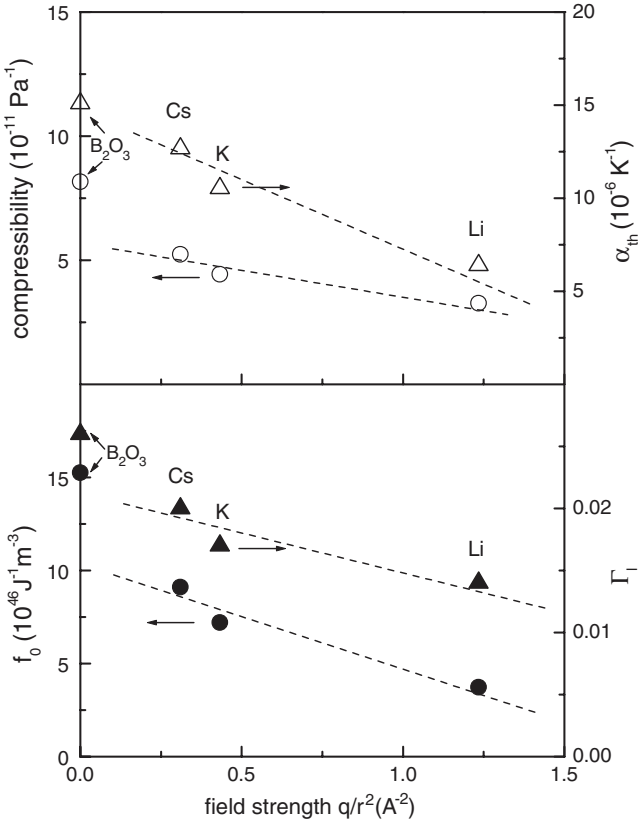

Figure 3. The dependences on the cationic field strength of: (a) the compressibility (inverse bulk modulus) (○) and the linear thermal expansion coefficient α_{th} (△), (b) the spectral density of asymmetries f_0 (●) and the anharmonicity coefficient Γ_l (▲). The values for pure glassy B_2O_3 are also included for comparison. The dotted lines are guides for the eye only.

In the context of the theoretical views [8, 24] linking both the one-phonon assisted tunnelling and the classical relaxation rates, the present ultrasonic study leads us to conclude that glasses having the same short range structure but different cation field strengths, as well as glasses having a structure modified by increasing addition of the same NMI [9], show that only a fraction of the relaxing centres experiences tunnelling motion.

4.2. Sound velocity

The rigidity of $(M_2O)_{0.14}(B_2O_3)_{0.86}$ glasses critically depends on the field strength of NMI: it increases with decreasing cation size leading to growth of both the bulk modulus B $(=\rho V_l^2 - \frac{4}{3}G)$ and the shear modulus G $(=\rho V_t^2)$ (table 1). Since at the fixed alkali oxide concentration of $x = 0.14$ the connectivity (defined as the number of bridging oxygens per network forming ion (NFI)) of the borate network has the constant value of 3.14, it results that the Coulombic interactions between the cations which occupy sites in the existing interstices and the charged tetrahedral $B\emptyset_4^-$ groups represent a substantial source for the stiffening of the glassy network.

As already observed in lithium borate glasses [9], the temperature dependences of the ultrasonic velocities in alkali borate glasses show a negative temperature coefficient in the

Table 1. Room temperature values of the density ρ, velocities of longitudinal (v_l) and transverse (v_t) ultrasonic waves, Debye temperature Θ_D, shear (G) and bulk (B) moduli, linear thermal expansion coefficient α_{th} and anharmonicity coefficient Γ_l in $(M_2O)_{0.14}(B_2O_3)_{0.86}$ glasses. The glass transition temperatures T_g are also included.

Samples	ρ (kg m^{-3})	T_g (K)	v_l (m s^{-1})	v_t (m s^{-1})	Θ_D (K)	G (GPa)	B (GPa)	α_{th} (10^{-6} K^{-1})	Γ_l
B_2O_3	1838	546	3367	1872	267	6.44	12.2	15.1	0.026
$(Cs_2O)_{0.14}(B_2O_3)_{0.86}$	2484	631	3578	1961	270	9.55	19.1	12.68	0.020
$(K_2O)_{0.14}(B_2O_3)_{0.86}$	2088	663	4228	2301	331	11.06	22.5	10.53	0.017
$(Li_2O)_{0.14}(B_2O_3)_{0.86}$	2071	697	5060	2851	427	16.83	30.5	6.5	0.014

Table 2. Values of the parameters related to the tunnelling (C_l and $\bar{P}\gamma_l^2$) and thermally activated relaxation (C_l^*, V_0, τ_0, and $f_0\gamma_l^2$) processes in $(M_2O)_{0.14}(B_2O_3)_{0.86}$ glasses.

Samples	C_l $\times 10^4$	$\bar{P}\gamma_l^2$ (10^7 J m^{-3})	γ (eV)	$\bar{P}$ (10^{45} J^{-1} m^{-3})	V_0/k_B (K)	C_l^* $\times 10^3$	τ_0^{-1} (10^{13} s^{-1})	$f_0\gamma_l^2$ (10^8 J m^{-3})	f_0 (10^{46} J^{-1} m^{-3})
B_2O_3	2.4[a]	0.52[a]	0.21[a]	4.5[a]	725	8.28	1.0	1.73	15.3
$(Cs_2O)_{0.14}$-$(B_2O_3)_{0.86}$	3.79	1.2	0.47	2.13	728	16.2	1.8	5.17	9.1
$(K_2O)_{0.14}$-$(B_2O_3)_{0.86}$	4.66	1.74	0.55	2.24	685	15.0	4.1	5.60	7.2
$(Li_2O)_{0.14}$-$(B_2O_3)_{0.86}$	6.61	3.5	0.63	3.44	550	7.17	2.5	3.8	3.7

[a] Values taken from [27].

whole investigated range, but with a larger slope at low temperatures. Like the acoustic attenuation, below 20 K the sound velocity is regulated by quantum mechanisms, with TLSs being mainly responsible [8], while for $T > 20$ K a transition to behaviours driven by classical activation over the potential barriers and by vibrational anharmonicity are expected [9]. The shape of the velocity curves between 20 and 120 K clearly indicates predominance of relaxation effects, while the nearly linear trend observed for higher temperatures is associated with the contribution of anharmonic effects. To describe the temperature behaviour of the longitudinal sound velocity V_l in the whole temperature range between 20 and 300 K it is sufficient to write an expression which covers both relaxation and anharmonic contributions:

$$\left(\frac{\Delta V_l}{V_{l,0}}\right) = \left(\frac{\Delta V_l}{V_{l,0}}\right)_{rel} + \left(\frac{\Delta V_l}{V_{l,0}}\right)_{anh} \tag{5}$$

where $\Delta V_l = V_l(T) - V_{l,0}$ and $V_{l,0}$ is the sound velocity at the lowest temperature in the experiment.

In the ADWP model, the dispersion ($T > 20$ K) can be well expressed as [10, 11]:

$$\left(\frac{\Delta V_l}{V_{l,0}}\right)_{rel} = -\frac{\gamma_i^2}{\rho V_l^2 k_B T}\int\int \mathrm{d}\Delta\, \mathrm{d}V f(\Delta) g(V) \sec h^2\left(\frac{\Delta}{2k_B T}\right)\frac{1}{1+\omega^2\tau^2}. \tag{6}$$

By applying the method of Gilroy and Phillips [11], described above, equation (6) can be reduced to the following form:

$$\left(\frac{\Delta V_l}{V_{l,0}}\right)_{rel} = \left(\frac{f_0\gamma^2}{\rho V_l^2}\right)\left[(\omega\tau_0)^\alpha - 1\right] = C^*\left[(\omega\tau_0)^\alpha - 1\right]. \tag{7}$$

Evaluation of the anharmonic contribution to the longitudinal sound velocity has been performed by using an extension of the quasiharmonic continuum model of Garber and

Granato [25] to isotropic materials [26]:

$$\left(\frac{\Delta V_l}{V_{l,0}}\right)_{\text{anh}} = \left(\frac{L}{L_0}\right)^{\frac{3}{2}} \left[1 - \Gamma_l F\left(\frac{T}{\Theta}\right)\right]^{\frac{1}{2}} - 1 \tag{8}$$

with

$$F\left(\frac{T}{\Theta}\right) = \left[3\left(\frac{T}{\Theta}\right)^4 \int_0^{\frac{\Theta}{T}} \frac{x^3\,\mathrm{d}x}{\mathrm{e}^x - 1}\right] \tag{9}$$

where L is the length of the sample, L_0 the length of the sample at $T = 0$ K, Θ the Debye temperature and $C_{11} = \rho V_l^2 = B + \frac{4}{3}G$. The anharmonicity coefficient Γ_l mainly depends on the mean acoustic-mode Grüneisen parameter $\gamma_{\text{G,el}}$. It has been assumed as temperature and frequency independent in the range between 120 and 300 K and in the limit of long wavelength (the regime of ultrasonic waves) [9].

Using the parameters obtained by the numerical evaluation of the relaxation loss (see table 2) in equation (7) and the room temperature values of Θ (see table 1) in equation (8), the temperature behaviours of the sound velocity have been evaluated by using Γ_l as the only parameter of the fit. The values of Γ_l are reported in table 1 and a typical fit of $\left(\frac{\Delta V_l}{V_{l,0}}\right)$ is shown by a continuous line in figure 2(b). Figure 3(b) shows that Γ_l decreases with increasing field strength (or decreasing cation size) in close correlation with the behaviour of the linear thermal expansion coefficient α_{th}, one of the markers of the vibrational anharmonicity. The striking similarity between the field strength behaviours of Γ_l and α_{th} implies that the long-wavelength acoustic modes do contribute substantially to the collective summations over the vibrational modes in borate glasses. In terms of a quite simplified view, the observed decrease of the anharmonicity with decreasing cation size is consistent with the structural picture of alkali borate glasses. At the fixed $X = 0.14$ concentration of alkali oxide (corresponding to a fixed number of $B\text{Ø}_4^-$ groups), the enhancement of the material stiffness with decreasing cation size is mainly due to the Coulombic interactions of M^+ modifier ions with the oxygen atoms of $B\text{Ø}_4^-$ groups. The Coulombic interactions are the origin of the restoring forces for the motions of oxygen atoms which become stronger with increasing cation field strength and lead to tighter structures having smaller thermal expansion coefficients. The effect of the restoring forces is to reduce the compressibility (inverse bulk modulus) and the expansion capability of the whole network with decreasing cation size (see figure 3(a)). It is believed that the anharmonic rattling of M^+ modifier ions within their local cages follows the short-time motions of M^+ ions in asymmetric binding potentials determined by their Coulombic interactions with oxygen atoms. The asymmetry of the potentials decreases with decreasing cation size, resulting in an overall lower anharmonicity of the vibrational modes.

5. Conclusions

Alkali borate glasses having the same local structure but hosting network-modifying ions with increasing sizes from Li^+ to Cs^+ exhibit an attenuation of ultrasound whose temperature behaviour is regulated by tunnelling systems below about 20 K and by thermally activated structural defects at higher temperatures. The magnitude of the attenuation depends strongly on the cation size in the regime of classical activation, revealing that, at variance with the tunnelling strength C, the relaxation strength C^* decreases with decreasing cation size exhibiting values which are more than one order of magnitude larger than those of C. The application of an asymmetric double-well potential model allows for quite a coherent linking between high temperature classical relaxation processes and low temperature quantum

effects observed in the acoustic behaviours of these borate glasses. Assuming that increasing temperature transforms the mechanisms of local mobility of the same defect states from tunnelling to classical activation, the evidence resulting from the different magnitudes of C and C^* leads to the conclusion that only a small fraction of the relaxing particles are involved in tunnelling local motions. The behaviour of the characteristics of the thermally activated relaxations with decreasing cation size can be explained by the following considerations:

(i) The relaxing centres are within the borate skeleton of these glasses, which are built on linked triangular borate units BO_3 and BO_4 charged tetrahedra, the latter being formed by the addition of the alkali oxide.

(ii) The Coulombic interactions between the modifying cations and the charged $B\emptyset_4^-$ tetrahedrons lead to a reduction in the number of internal degrees of freedom of the locally mobile units, hindering their local motions between different configurations. The effect of these interactions becomes larger with decreasing cation size or increasing field strength, enhancing the degree of hindrance and causing the observed decrease of the number of relaxing units.

Classical activation also regulates the sound velocity between 20 and 120 K, whereas the vibrational anharmonicity is the dominant mechanism at higher temperatures. The anharmonicity of the glassy network decreases with increasing field strength of the modifier ion, in close correlation with the parallel reduction of the local molecular mobility.

The totality of the observations concerning the defect states in borate glasses leads to conclude that, differently from classical relaxing states, tunnelling TLSs confirm their universal character as inherent to the glassy state. They cause an internal friction Q^{-1}_{plateau} which lies in the range between 10^{-4} and 10^{-3} (corresponding to a ratio between the wavelength and the mean free path of sound waves ranging between 10^{-3} and 10^{-2}), independent of structural changes and of bond strengths characterizing the glassy network.

References

[1] Zeller R C and Pohl R O 1971 *Phys. Rev.* B **4** 2029
Pohl R O 1981 *Amorphous Solids* vol 24, ed W A Phillips (Berlin: Springer) p 27
[2] Anderson A C 1981 *Amorphous Solids* vol 24, ed W A Phillips (Berlin: Springer) p 65
[3] Hunklinger S and v Schickfus M 1981 *Amorphous Solids* vol 24, ed W A Phillips (Berlin: Springer) p 81
[4] Pohl R, Liu X and Thompson E 2002 *Rev. Mod. Phys.* **74** 991 and references therein
[5] Anderson P W, Halperin B I and Varma C M 1972 *Phil. Mag.* **25** 1
[6] Phillips W A 1972 *J. Low Temp. Phys.* **7** 351
[7] Neu P and Würger A 1994 *Europhys. Lett.* **27** 457
[8] Rau S, Enss C, Hunklinger S, Neu P and Würger A 1995 *Phys. Rev.* B **52** 7179
[9] Carini G Jr, Carini G, D'Angelo G, Tripodo G, Bartolotta A and Salvato G 2005 *Phys. Rev.* B **72** 14201
[10] Jackle J, Pichè L, Arnold W and Hunklinger S 1976 *J. Non-Cryst. Solids* **28** 365
[11] Gilroy K S and Phillips W A 1981 *Phil. Mag.* B **43** 735
[12] Bray P J 1999 *Inorg. Chim. Acta* **289** 158
Zhong J and Bray P J 1989 *J. Non-Cryst. Solids* **111** 67
[13] Ratai E M, Janssen M, Epping J D, Chan J C C and Eckert H 2003 *Phys. Chem. Glasses* **44** 45
[14] Kryssikos G D, Kamitsos E I and Karakassides M A 1990 *Phys. Chem. Glasses* **31** 109
[15] Kamitsos E I 2003 *Phys. Chem. Glasses* **44** 79
[16] Swenson J, Borjesson L and Howell W S 1995 *Phys. Rev.* B **52** 9310
[17] Jackle J 1972 *Z. Phys.* **257** 212
[18] Parshin D A 1994 *Phys. Rev.* B **49** 9400
Parshin D A 1994 *Phys. Solid State* **36** 991 and references therein
[19] Carini G, Cutroni M, Federico M and Tripodo G 1988 *Phys. Rev.* B **37** 7021
[20] Tielbürger D, Merz R, Ehrenfels R and Hunklinger S 1992 *Phys. Rev.* B **45** 2750

[21] Bonnet J P 1991 *J. Non-Cryst. Solids* **127** 227
[22] Shannon R D 1976 *Acta Crystallogr.* A **32** 751
[23] Kühn R and Horstmann U 1997 *Phys. Rev. Lett.* **78** 4067
[24] Phillips W A 1989 *Phonons* vol 89, ed S Hunklinger, W Ludwig and G Weiss (Singapore: World Scientific) p 367
[25] Garber J A and Granato A V 1975 *Phys. Rev.* B **11** 3990
[26] Claytor T N and Sladek R J 1978 *Phys. Rev.* B **18** 5842
[27] Devaud M, Prieur J Y and Wallace W D 1983 *Solid State Ion.* **9/10** 593